IL NUOVO CIMENTO **45 C** (2022) 51
DOI 10.1393/ncc/i2022-22051-6

COLLOQUIA: IWM-EC 2021

Understanding isospin transport ratio: Influence of fast emissions and statistical de-excitation

A. CAMAIANI(*) for the INDRA+FAZIA COLLABORATION

Instituut voor Kern- en Stralingsfysica, K.U. Leuven - Celestijnenlaan 200D, B-3001 Leuven, Belgium

received 12 May 2022

Summary. — We report on one of the main techniques used to estimate the neutron-proton equilibration in heavy-ion collision: the so-called isospin transport ratio, which is expected to bypass any perturbations introducing a linear transformation of the chosen observable. In this proceeding, we will focus on the perturbations introduced by fast and statistical emissions that occur after the projectile-target separation, when the equilibration is already established. We chose ^{40,48}Ca+^{40,48}Ca at 35 MeV/nucleon as a bench test, adopting a full model scheme based on the Antisymmetrized Molecular Dynamics models coupled with several statistical codes. Using the n-p ratio (N/Z) of the Quasi-Projectile as an isospin sensitive observable, we observed a perturbation introduced by the statistical de-excitation of the primary fragments at relatively low excitation energies (below 2 MeV/nucleon), while fast and more dynamical emissions after the projectile-target separation introduced some perturbation once the centrality of the events increased.

1. – Introduction

Heavy-ion collisions in the Fermi energy domain (25–50 MeV/nucleon) are a good probe to shed light on the nuclear Equation of State (nEoS), which its knowledge is still far to be satisfactory [1]. In particular, the investigation of the so-called isospin dynamics, *i.e.*, the nucleon exchange between projectile and target during the collision, could provide reliable information on the Taylor expansion coefficient of the asymmetric term of the nEoS, the so-called symmetry energy [2]. Two of the most interesting phenomena are the isospin diffusion, *i.e.*, the nucleon flow due to an initial unbalance on the proton and neutron content between projectile and target, and the isospin drift, *i.e.*, the nucleon migration towards a low-density region that can develop during the collision. During the years, many efforts have been spent to investigate both isospin diffusion [3-6]

(*) E-mail: alberto.camaiani@kuleuven.be

and isospin drift [7-11] trying to constrain the first and/or higher-order terms of the symmetry energy.

Focusing on the isospin diffusion, one of the most powerful tools to investigate on is the isospin transport ratio (also known as the imbalance ratio), which allows estimating the neutron-proton equilibration degree in a model independent way [12]. Such a technique exploits the information extracted with an isospin sensitive observable (X) extracted from three systems differing on the initial isospin content: two symmetric systems, a n-rich and a n-deficient one, used as reference since where no isospin diffusion develops, and an asymmetric system where isospin diffusion is expected to develop. The isospin transport ratio normalizes the observation on the asymmetric system to the two symmetric ones: $R(X) = \frac{2X - X^{nrich} - X^{ndef}}{X^{nrich} - X^{ndef}}$. For the two symmetric systems, $R(X)$ is normalized to $+1$ and -1 for the n-rich and n-deficient system, respectively. Moreover, if the chosen observable linearly depends on the isospin, $R = 0$ represents the full n-p equilibration [12].

According to Rami *et al.* [12], if the three reactions are investigated under identical experimental conditions, the ratio is insensitive to systematic uncertainties due to the apparatus, fast dynamical emission and secondary decay, as well Coulomb effects [13-16]. More generally, this method bypasses any effect, which introduces a linear transformation (F_L) on the adopted observable X, *i.e.*, $R[F_L(X)] = R(X)$. Instead, nonlinear transformations (F_{NL}) introduce a deformation of the isospin transport ratio, therefore $R[F_{NL}(X)] \neq R(X)$.

Since the introduction of the isospin transport ratio, several isospin sensitive observables have been used, as the $A = 7$ mirror nuclei ratio [13], the isoscaling parameter and the $A = 3$ and 7 isobaric ratio [14, 15, 17]. As the isospin sensitive observable, in this proceeding we will select the neutron to proton ratio (N/Z) of the Quasi-Projectile (QP) observed in binary dissipative collisions. Indeed, such a variable other than mass spectrometer can be now accessed by array detectors as FAZIA [18,19] and NIMROD [20]. We will focus on the perturbations introduced by the fast dynamical emission and statistical decay of the produced hot fragments, while effects more related to the nuclear interaction such as mean-field, in-medium cross section, and dynamical cluster production can be found elsewhere [16].

2. – Investigation approach

As a bench test we adopted ^{40,48}Ca + ^{40,48}Ca at 35 MeV/nucleon, since it allows scanning a large range on N/Z with stable beams, from $N/Z = 1$ for ^{40}Ca to $N/Z = 1.4$ for the ^{48}Ca. Moreover, it is a common system investigated by several research groups, as CHIMERA [21, 22], INDRA + VAMOS [23], and also recently by the FAZIA Collaboration [6] aiming at a direct measurement of isospin equilibration with isospin transport ratio.

We assumed a two-step process, as commonly done in nuclear reactions in the Fermi domain [7, 24, 25]. According to the scheme reported in fig. 1, once a projectile and a target with a different n-p content collide, a nucleon diffusion develops between them in order to restore the initial unbalance; at the separation time (t_{dic}), the equilibration degree of the emerging excited, and most likely deformed, QP and QT is established and they undergo through fast dynamical emissions and then a statistical de-excitation, once they reached the thermodynamical equilibration.

In order to reproduce such a scenario, we adopted a model-based approach: we used the Antisymmetrized Molecular Dynamics (AMD) transport model [26] to simulate the dynamical phase up to 500 fm/c from the onset of the interaction; this is a sufficiently

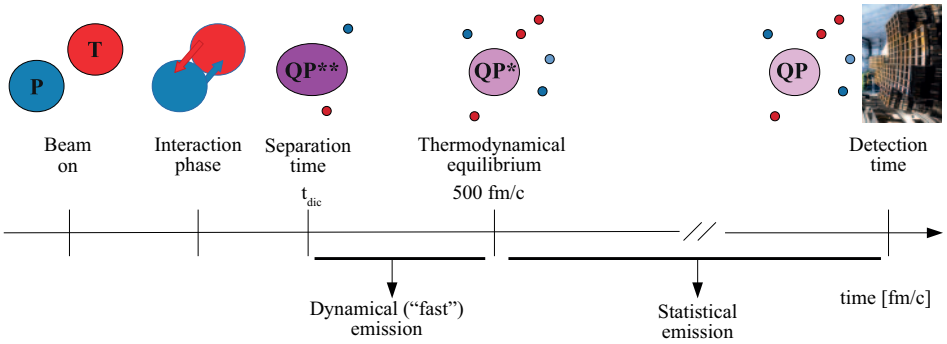

Fig. 1. – Schematic representation of a collision of a n-rich projectile (P) and a n-deficient target (T). Once they collide, a net n-p flow develops up to the separation to restore the initial unbalance. After the separation time, only the Quasi-Projectile phase space is shown. The QP initially goes through dynamical fast emission and, once the thermodynamical equilibrium is reached, it decays in a statistical way.

long time to ensure that the dynamical phase is concluded when the primary ejectiles have reached the thermodynamical equilibrium, and to ensure that the fragment mutual Coulomb repulsion is negligible [25]. At this time, AMD has been coupled with several statistical codes, GEMINI++ (GEM++) [27], GEMINIF90 (GEMF90) [28], and SIMON [29], in order to reproduce the effect of the statistical de-excitation.

For each system, we produced approximately 40000 events, with a triangular distribution of the impact parameter up to the grazing value (b_{gr}). We will focus on binary reactions, *i.e.*, peripheral and semiperipheral events with $b_{red} = b/b_{gr} \geq 0.4$. The event selection is performed at the end of the statistical stage; the QP and QT remnants from binary collisions are selected as $Z \geq 12$, only accompanied by neutrons, light charged particles (H and He ions), and intermediate mass fragments, produced during the decay path. The selected sample represents 62% of the whole statistics and 98% of the events in the selected range of centrality.

As the isospin sensitive observable, we adopted the average neutron-proton ratio ($\langle N/Z \rangle$, eq. (2) of ref. [30]). Eventually, to follow the equilibration degree as a function of the reaction centrality we chose as ordering variable the excitation energy per nucleon (E^*/A) of the QP evaluated at 500 fm/c. This latter choice is motivated by the fact that E^*/A is one of the key-parameters of the statistical decay.

3. – Results

In order to evaluate the effects of the statistical de-excitation and dynamical fast emission on the estimation of the equilibration degree, we have to compare the isospin transport ratio at different times, keeping in mind that the true equilibration is the one measured at the separation time, t_{dic} according to fig. 1.

We can start exploring the effect of the statistical emissions. In this sense, in order to distinguish the effect of the statistical decay from that of a more prompt emission, we can compare the equilibration degree obtained at the end of the afterburner with that from primary QP at 500 fm/c (the end of the dynamical phase according to our modelization). In this way, any difference is attributable to the statistical decay only. Results are reported in fig. 2(a), (b) using the three aforementioned statistical codes as afterburners. Colors and symbols according to the legend in panel (a).

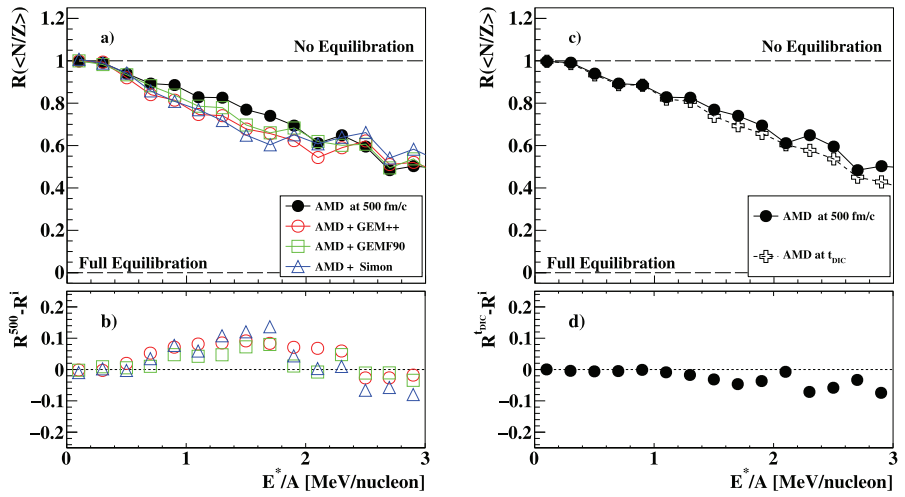

Fig. 2. – (a) Isospin transport ratio for the AMD primary QP at 500 fm/c (solid circles) and at the end of the statistical de-excitation. (b) Differences in the equilibration degree of the QP remnant with respect to that obtained at 500 fm/c (open symbols). (c) Isospin transport ratio for the AMD primary QP at the separation time t_{dic} (open crosses) and at 500 fm/c. (d) Differences in the equilibration degree of the QP at t_{dic} with respect to that obtained at 500 fm/c (solid circles). Statistical errors are smaller than the marker size. Lines are drawn to guide the eyes.

Both at 500 fm/c (black solid) and at the end of the statistical decay, the system evolves from $R = 1$ (no equilibration) downwards as the E^*/A increases. As expected, the system evolves towards the charge equilibrium once the collision becomes more dissipative [2, 6, 16]. However, some differences between the values at 500 fm/c and those at the end of the de-excitation appear. However, such discrepancies are not related to the Monte Carlo code used to simulated the statistical stage, as they are present both in GEM++, GEMF90, and SIMON. Such a difference in the equilibration degree can be better seen by computing the difference between the equilibration at 500 fm/c at that at the end of the de-excitation (fig. 2(b)). We observe a discrepancy up to 0.1 in the range 0.6–2.2 MeV/nucleon, thus pointing towards some perturbation introduced by the statistical decay and not bypassed by the isospin transport ratio in this excitation energy range.

We can shed light on the nature of the transformation, by performing some dedicated statistical decay simulation. Let's define as F the transformation of N/Z representing the effects of the evaporation. F is a function of the neutron number N, atomic number Z, angular momentum J, level density parameter a, and excitation energy per nucleon E^*/A, *i.e.*, the inputs that rule the statistical decay of a nucleus. We produced two sets of GEMINI++ simulations for several specific hot nuclei fixing their mass: the first with $A = 40$ nuclei, the second with $A = 48$, thus scanning the whole N/Z range. The chosen nuclei are labeled in the central panel of fig. 3(b). Correlating the initial N/Z value with the final one we can extract the shape of the transformation F, as reported in fig. 3 for three different bins of E^*/A. It is likely true that once the E^*/A increases, the transformation introduced by the statistical decay becomes linear, thus it can be bypassed by the isospin transport ratio. This finding confirms the previous observation.

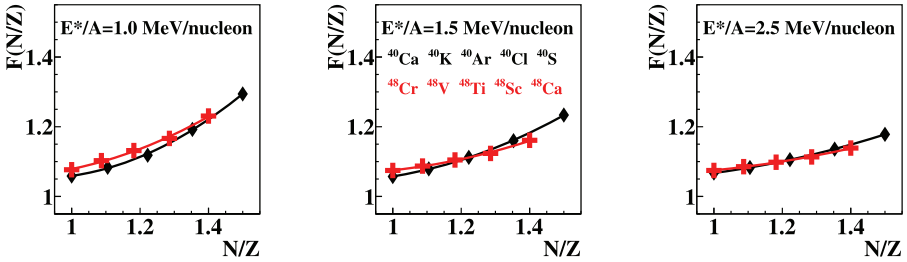

Fig. 3. – GEMINI++ simulation for two different sets of nuclei, $A = 40$ (solid black diamond) and $A = 48$ (solid red crosses). In the picture, correlations between the neutron-to-proton ratio obtained at the end of the evaporation ($F(N/Z)$) and that of the input nuclei (N/Z) are shown, for three different values of E^*/A as quoted.

The non-linearity of the transformation at low excitation energy could be due to structure effects, since it is well known that they affect the particle emission at E^*/A [31-33]. Further studies are ongoing.

Finally, we can now move to the investigation of the effects introduced by some more dynamic emissions. In particular, we focus on the emissions that occur between the projectile-target separation time (t_{dic}) and 500 fm/c, *i.e.*, within the only AMD model. For each event selected at the end of the statistical stage, we can go back in time until a unique system with a mass and charge comparable with the interacting projectile-target. Such a time defines t_{dic}. For better accuracy and consistency, going back in time we require that for each step the size of the identified QP be not less than that at the previous time step. The comparison between the equilibration degree measured at t_{dic} and 500 fm/c is reported in fig. 2(c), where the R values at t_{dic} are reported with open crosses. The trend as a function of E^*/A is very similar between the equilibration degree at t_{dic} and at 500 fm/c, and some slight differences arise for $E^*/A > 2$ MeV/nucleon, as we can better see computing the difference in fig. 2(d). As the excitation energy per nucleon increases, fast emissions introduce non-linear distortions that cannot be fully recovered by the isospin transport ratio. This is reasonable because once we are selecting events with larger E^*/A, we are moving towards more central events, where the probability of such fast emission increases [30].

4. – Conclusion

We investigated the effects introduced by statistical and dynamical emissions on the estimation of the equilibration degree via isospin transport ratio. We adopted a full model scheme, performing Antisymmetrized Molecular Dynamics model simulation, coupled with several statistical models, on Ca+Ca reaction at 35 MeV/nucleon.

We compared the equilibration degree at three different times, namely the end of the statistical stage, the end of the dynamical phase (500 fm/c) where we assumed that the primary fragments produced by AMD have reached the thermodynamical equilibrium, and the end of the interaction between projectile and target when the real equilibration degree is established.

The statistical de-excitation produces a transformation of the Quasi-Projectile N/Z values which tends to be linear at relatively high excitation energies thus not affecting the isospin transport ratio. In the present case this corresponds to excitation energies above

2 MeV/nucleon, which corresponds on average of events with reduced impact parameter $b_{red} < 0.8$.

On the other hand, the particle emission just after the projectile-target separation and the end of the dynamical phase (500 fm/c) perturb the real n-p equilibration degree at an extent that increases with the collision violence (decrease of the impact parameter). In particular, their effect on the isospin transport ratio becomes significant for semi-central events, approximately for $b_{red} < 0.8$. For more peripheral reactions, at least for these reactions, the fast emissions are negligible (and so is their effect on the isospin transport ratio).

The detailed description of this study is published elsewhere [30].

* * *

Thanks are due to INFN-CNAF and GARR for providing the computing resources to perform Monte Carlo simulations.

REFERENCES

[1] Magueron J. *et al.*, *Phys. Rev. C*, **97** (2018) 025805.
[2] Baran V. *et al.*, *Phys. Rep.*, **410** (2005) 335.
[3] Piantelli S. *et al.*, *Phys. Rev. C*, **96** (2017) 034622.
[4] Piantelli v. *et al.*, *Phys. Rev. C*, **103** (2021) 014603.
[5] May L. W. *et al.*, *Phys. Rev. C*, **98** (2018) 044602.
[6] Camaiani A. *et al.*, *Phys. Rev. C*, **103** (2021) 014605.
[7] De Filippo E. *et al.*, *Phys. Rev. C*, **86** (2012) 014610.
[8] Piantelli S. *et al.*, *Phys. Rev. C*, **101** (2020) 034613.
[9] Camaiani A. *et al.*, *Nuovo Cimento C*, **41** (2018) 172.
[10] Jedele A. *et al.*, *Phys. Rev. Lett.*, **118** (2017) 062501.
[11] Rodriguez Manso A. *et al.*, *Phys. Rev. C*, **95** (2017) 044604.
[12] Rami F. *et al.*, *Phys. Rev. Lett.*, **84** (2000) 1120.
[13] Liu T. X. *et al.*, *Phys. Rev. C*, **76** (2007) 034603.
[14] Tsang M. B. *et al.*, *Phys. Rev. Lett.*, **92** (2004) 062701.
[15] Tsang M. B. *et al.*, *Phys. Rev. Lett.*, **102** (2009) 122701.
[16] Coupland D. D. S. *et al.*, *Phys. Rev. C*, **84** (2011) 054603.
[17] Sun Z. Y. *et al.*, *Phys. Rev. C*, **82** (2010) 051603.
[18] Bougaulté R. *et al.*, *Eur. Phys. J. A*, **50** (2015) 47.
[19] Valdré S. *et al.*, *Nucl. Instrum. Methods A*, **930** (2010) 27.
[20] Wuenschel S. *et al.*, *Nucl. Instrum. Methods A*, **604** (2009) 578.
[21] Lombardo I. *et al.*, *Phys. Rev. C*, **84** (2011) 024613.
[22] Cardella G. *et al.*, *Phys. Rev. C*, **85** (2012) 064609.
[23] Quentin Fable, Université de Caen Normandie, PhD Thesis (2018).
[24] Tian G. *et al.*, *Phys. Rev. C*, **97** (2018) 034610.
[25] Piantelli S. *et al.*, *Phys. Rev. C*, **99** (2019) 064616.
[26] Ono A., *Prog. Part. Nucl. Phys.*, **105** (2019) 139.
[27] Charity R., *Phys. Rev. C*, **82** (2010) 014610.
[28] Charity R. *et al.*, *Nucl. Phys. A*, **483** (1988) 371.
[29] Durand D., *Nucl. Phys. A*, **541** (1992) 266.
[30] Camaiani A.*et al.*, *Phys. Rev. C*, **102** (2020) 044607.
[31] Camaiani A. *et al.*, *Phys. Rev. C*, **97** (2018) 044607.
[32] Morelli L. *et al.*, *Phys. Rev. C*, **99** (2019) 054610.
[33] Bruno M. *et al.*, *J. Phys. G*, **46** (2019) 12510.